Source: HANDBOOK OF OPTICS

PART 6

IMAGING DETECTORS

Downloaded from Digital Engineering Library @ McGraw-Hill (www.accessengineeringlibrary.com)
Copyright © 2010 The McGraw-Hill Companies. All rights reserved.
Any use is subject to the Terms of Use as given at the website.

Downloaded from Digital Engineering Library @ McGraw-Hill (www.accessengineeringlibrary.com)
Copyright © 2010 The McGraw-Hill Companies. All rights reserved.
Any use is subject to the Terms of Use as given at the website.

Source: HANDBOOK OF OPTICS

29 PHOTOGRAPHIC FILMS

Joseph H. Altman
Institute of Optics
University of Rochester
Rochester, New York

29.1 GLOSSARY

A	area of microdensitometer sampling aperture
a	projective grain area
D	optical transmission density
D_R	reflection density
DQE	detective quantum efficiency
$d(\mu)$	diameter of microdensitometer sampling aperture stated in micrometers
E	irradiance/illuminance (depending on context)
$\mathcal{G}$	Selwyn granularity coefficient
g	absorbance
H	exposure
IC	information capacity
M	modulation
M_e	angular magnification
m	lateral magnification
NEQ	noise equivalent quanta
$P(\lambda)$	spectral power in densitometer beam
Q'	effective Callier coefficient
q	exposure stated in quanta/unit area
R	reflectance
S	photographic speed
$S(\lambda)$	spectral sensitivity
S/N	signal-to-noise ratio of the image
T	transmittance
$T(\nu)$	modulation transfer factor at spatial frequency ν

Downloaded from Digital Engineering Library @ McGraw-Hill (www.accessengineeringlibrary.com)
Copyright © 2010 The McGraw-Hill Companies. All rights reserved.
Any use is subject to the Terms of Use as given at the website.

t	duration of exposure
WS(ν)	value of Wiener (or power) spectrum for spatial frequency ν
γ	slope of D-log H curve
ν	spatial frequency
$\rho(\lambda)$	spectral response of densitometer
$\sigma(D)$	standard deviation of density values observed when density is measured with a suitable sampling aperture at many places on the surface
$\sigma(T)$	standard deviation of transmittance
$\phi(\tau)$	Autocorrelation function of granular structure

29.2 STRUCTURE OF SILVER HALIDE PHOTOGRAPHIC LAYERS

The purpose of this chapter is to review the operating characteristics of silver halide photographic layers. Descriptions of the properties of other light-sensitive materials, such as photoresists, can be found in Ref. 4.

Silver-halide-based photographic layers consist of a suspension of individual crystals of silver halide, called *grains*, dispersed in gelatin and coated on a suitable "support" or "base." The suspension is termed an *emulsion* in the field. The grains are composed of AgCl, AgClBr, AgBr, or AgBrI, the listing being in order of increasing sensitivity. Grain size ranges from less than 0.1 μm ("Lippmann" emulsions) to 2 to 3 μm, depending on the intended use of the coating. The number of grains per square centimeter of coating surface is usually very large, of the order of 10^6 to 10^8 grains/cm^2. The weights of silver and gelatin coated per unit area of support vary depending on intended use; usually both fall in the range 1 to 10 g/m^2. The silver-to-gel ratio may also vary depending on intended use. Typically, the emulsion may be about 30 to 40 percent silver by weight, but some special-purpose materials, such as films to record Schumann-wavelength-region radiation, contain very little gelatin.

For modern materials, both the emulsion and the coating structure can be very complex. The emulsion layer is much more than silver halide in gelatin, containing additional agents such as hardeners, antifoggants, fungicides, surfactants, static control agents, etc. Likewise, the coating structure may be very complex. Even some black-and-white materials consist of layers of two different emulsions coated one over the other and a thin, clear layer of gelatin is often coated over the emulsion(s) to provide some mechanical protection. In the case of color films, as many as 15 layers may be superimposed, some of them of the order of 1 μm thick. The thickness of the complete coating varies from about 3 μm to about 25 μm in normal films.

Commercially available emulsions are coated on a variety of glass, plastic (film), and paper supports (or "bases"). Glass is used for mechanical rigidity, spatial stability, or surface flatness.

Two different types of plastic are available commercially as film supports: cellulose acetate and polyethylene terephthalate (trade names "Cronar," "Estar," and "Mylar"). Of the two types, Mylar is superior in strength, flexibility, and spatial stability. However, the material is birefringent and its physical properties may be different in orthogonal directions. Also, these directions may not be aligned with the length or width of the sample. The anisotropic properties arise from the method of manufacture. Although not as tough as Mylar, cellulose acetate is, of course, fully adequate for most purposes. Also, this material is isotropic and easier to slit and perforate. Typical supports for roll films are around 4 mils (102 μm) thick, and for sheet films, 7 mils (178 μm), and other thicknesses are available. Most films are also coated on the back side of the support. The "backing" may be a layer of clear gelatin applied for anticurl protection, or of gelatin dyed with a dye that bleaches during processing, and provides both anticurl and antihalation protection. Lubricants and antistatic agents may also be coated, either on the front or back of the film. Properties of supports are discussed in Ref. 1.

Downloaded from Digital Engineering Library @ McGraw-Hill (www.accessengineeringlibrary.com)
Copyright © 2010 The McGraw-Hill Companies. All rights reserved.
Any use is subject to the Terms of Use as given at the website.

29.3 GRAINS

The grain is the radiation-sensing element of the film or plate. It is a face-centered cubic crystal, with imperfections in the structure. For the most part, the grains act as independent receptors. In general, the larger grains are faster. The properties of the individual grains are controlled by the precipitation conditions and the after-precipitation treatment. Details of these matters are proprietary, but some discussion is given in Refs. 2 and 3. From the user's standpoint, the important fact is that when the grain is exposed to sufficient radiation it forms a "latent-image speck" and becomes *developable* by a solid-state process called the "Gurney-Mott mechanism." An excellent review of grains and their properties is given by Sturmer and Marchetti in chap. 3 of Ref. 4.

29.4 PROCESSING

The exposed halide layer is converted to a usable image by the chemical processes of development and fixation.

Development consists of reducing exposed crystals from silver halide to metallic silver, and a developing agent is an alkaline solution of mild reducer that reduces the grains having latent image specks, while not attacking the unexposed grains. Generally, once development starts the entire grain is reduced if the material is allowed to remain in the developer solution. Also, in most cases adjacent grains will not be affected, although developers can be formulated that will cause adjacent grains to be reduced ("infectious developers"). The number of quanta that must be absorbed by a grain to become developable is relatively small, of the order 4 to 40, while the developed grain contains on the order of 10^6 atoms. The quantum yield of the process is thus very high, accounting for the speed of silver-based materials.

The remainder of the process consists essentially of removing the undeveloped halide crystals which are still light-sensitive. The "fixer" is usually an acid solution of sodium thiosulfate $Na_2S_2O_3$, called "hypo" by photographers. The fixing bath usually serves as a gelatin hardener also. The thiosulfate reacts with the halide of the undeveloped grains to form soluble silver complexes, which can then be washed out of the emulsion layer. It is worth noting that proper washing is essential for permanent images. Additional treatments to promote permanence are available. Processing is discussed in detail in Refs. 2, 3, and 5, and image permanence in Ref. 6.

The exposed and processed silver halide layer thus consists of an array of grains of metallic silver, dispersed in a gelatin matrix. In color films, the silver is removed, and the "grains" are tiny spheres of dyed gelatin (color materials will be discussed below). Either type of grain acts as an absorber; in addition, the metallic silver grains act as scatterers. The transmittance or reflectance of the layer is thus reduced and, from the user's standpoint, this change constitutes the response of the layer.

29.5 EXPOSURE

From fundamental considerations it is apparent that the dimensions of exposure must be energy per unit area. Exposure H is defined by

$$H = Et \tag{1}$$

where t is the time for which the radiation is allowed to act on the photosensitive layer, and therefore E must be the irradiance on the layer. The symbol H is used here for exposure in accordance with international standards, but it should be noted that in many publications, especially older ones, E is used for exposure and I for irradiance, so that the defining expression for exposure becomes $E = It$.

Strictly speaking, H and E in Eq. (1) should be in radiometric units. However, photographic exposures are customarily stated not in radiometric but in photometric units. This is done mostly

Downloaded from Digital Engineering Library @ McGraw-Hill (www.accessengineeringlibrary.com)
Copyright © 2010 The McGraw-Hill Companies. All rights reserved.
Any use is subject to the Terms of Use as given at the website.

for historical reasons; the English scientists Hurter and Driffield, who pioneered photographic sensitometry in 1891, measured the incident flux in their experiments in lumen per square meter, or lux. Their unit of exposure was thus the lux-second (old term, meter-candle-second). Strictly speaking, of course, weighting the incident flux by the relative visibility function is wrong or at least unnecessary, but in practice it works well enough because in most cases the photographer wishes to record what he or she sees, i.e., the visible spectrum. Conversion between radiometric and photometric units is discussed by Altman, Grum, and Nelson.[7]

Also, it should be noted that equal values of the exposure product (Et) may produce different outputs on the developed film because of a number of *exposure effects* which are described in the literature.[8] A complete review of radiometry and photometry is given in Chap. 34 in this volume of the *Handbook*.

29.6 OPTICAL DENSITY

As noted above, the result of exposure and processing is a change in the transmittance or reflectance of the layer. However, in photography, the response is usually measured in terms of the *optical density*, hereafter called the "density" in this chapter. For films (transmitting samples), density is defined by

$$D = -\log T = \log 1/T \tag{2}$$

where T is the transmittance. (Note: throughout this chapter, "log" indicates the base-10 logarithm.) For either silver grains or color grains, the *random dot* model of density predicts that

$$D = 0.434nag \tag{3}$$

where n = the number of grains per unit area of surface
a = the average projective grain area
g = the absorbance of the grain

Absorbance in turn is defined as $g = 1 - (T + R)$ where T and R are the transmittance and reflectance of the grain. For silver grains, the absorbance is taken as unity. The above expression, sometimes known as "Nutting's law," is based on a geometric approach, and does not take into account any scattering by the grains. However, of course, opaque silver particles on a clear background will act as scatterers, and in fact multiple scattering usually occurs in developed silver layers. This produces an increase in the density of such layers by a factor of 2 to 3 times from that predicted by Nutting's law. For color films, the refractive index of the gelatin in the dyed spheres is only negligibly different from that of the surround so that such layers are not scatterers. Even in the case of silver films, however, Nutting's law provides a useful model. Since for a given population of grains a and g will remain effectively constant, the law states that density should vary as the number of grains per unit area of surface. This fact is easily verified with a microscope.

Transmission Density

Transmission density is measured in a densitometer. It is worth noting that the device actually measures the transmittance of the sample and then displays the negative log of the result. In a normal or *macro* densitometer the sampling aperture area A is typically 1 mm^2 or more in size. When A is small, say, 0.1 mm^2 or less, the device becomes a *micro* densitometer. Microdensitometers present special problems and will be discussed below.

Because the scattered light may not reach the sensor of the densitometer when silver layers are measured, it is necessary to specify the angular subtenses of both the incident (influx) and emergent (efflux) beams at the sample. Clearly, if scattered light is lost to the sensor, the indicated density of the sample will *increase*. Four types of transmission density are described in an ISO standard,[9] of

Downloaded from Digital Engineering Library @ McGraw-Hill (www.accessengineeringlibrary.com)
Copyright © 2010 The McGraw-Hill Companies. All rights reserved.
Any use is subject to the Terms of Use as given at the website.

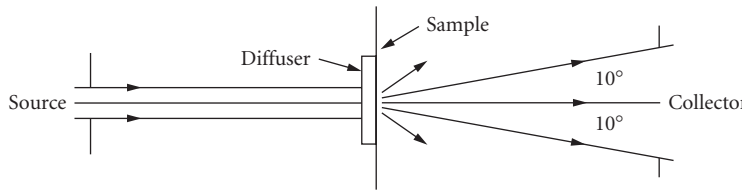

FIGURE 1 Optical system for measuring ISO/ANSI diffuse density with a 20° collection angle. (*Reprinted courtesy Eastman Kodak Co. © Eastman Kodak Co.*)

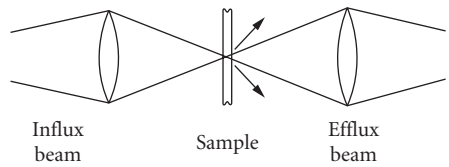

FIGURE 2 Optical conditions for projection density measurement.

which two are principally important to the user. The first of these is *diffuse density*, which is diagrammed in Fig. 1. As can be seen, a collimated incident beam illuminates an opal glass diffuser. The emulsion side of the sample is placed in contact with this diffuser, and the flux contained within a cone angle of ±10° is collected and evaluated by the sensor. The reverse of this arrangement yields the same density values and is also permitted by the standard. This is the type of density normally measured in practice. Physically, it corresponds to the conditions of contact printing.

The other case that is important in practice is projection density, which is diagrammed in Fig. 2. This case simulates the use of the layer in an optical system. As the figure shows, light is lost to the efflux system in projection density, the exact amount depending on the numerical aperture of the optics involved and the scattering characteristics of the sample. Thus, the projection density of a silver film is usually greater than the diffuse density. The effective Callier coefficient Q' may be defined by

$$Q' = \frac{\text{project density}}{\text{diffuse density}} \tag{4}$$

This factor can be measured experimentally. For silver films and *f*/2 optics, $Q' \approx 1.3$; for color films $Q' \approx 1.0$.

Nonneutral (Color) Density

In many cases, silver densities can be treated as neutrals. For dye densities, i.e., color films, measured density depends on the spectral characteristics of both the dye and the densitometer. The spectral response of the instrument is given by

$$\rho_\lambda = P_\lambda S_\lambda F_\lambda \tag{5}$$

where ρ_λ = the response at wavelength λ
P_λ = the power in the densitometer beam at λ
S_λ = the spectral sensitivity of the sensor at λ
F_λ = the transmittance of the densitometer optics at λ, specifically including any filters placed in the densitometer beam

Downloaded from Digital Engineering Library @ McGraw-Hill (www.accessengineeringlibrary.com)
Copyright © 2010 The McGraw-Hill Companies. All rights reserved.
Any use is subject to the Terms of Use as given at the website.

The measured density of a nonneutral layer is then

$$D = \log\left[\frac{\int_{\lambda_1}^{\lambda_2} \rho_\lambda d\lambda}{\int_{\lambda_1}^{\lambda_2} \rho_\lambda T_\lambda d\lambda}\right] \tag{6}$$

where T_λ is the transmittance of the layer at wavelength λ, and the wavelength limits are set by the distributions. The response ρ_λ of the system is adjusted to be equal to that of the readout device with which the film is to be used.

Thus, for example, if the sample is to be viewed by an observer, ρ_λ is made equal to the visibility function, and the resulting measurement is called visual density, etc. Instrument responses have been standardized for sensitometry of color films.[10]

Reflection Density

When the emulsion is coated on paper the density is measured by reflection. Reflection density is then defined by

$$D_R = -\log R \tag{7}$$

where R is reflectance, measured under suitable geometric conditions. The measurement of reflection density is also described in the standards literature.[11]

29.7 THE D-LOG H CURVE

In routine sensitometry, samples receive a series of exposures varying by some constant factor, such as ×2 or $\times\sqrt{2}$. After processing, the measured densities are plotted against the common logarithm of the exposures that produced them. The resulting curve is known as the "D-log H curve," or the "H & D" curve (after Hurter and Driffield, the previously mentioned pioneers in the field). A typical D-log H curve is shown in Fig. 3.

As shown, the curve is divided into three regions, known as the "toe," "straight-line portion," and "shoulder," respectively. The fact that an appreciable straight-line portion is found in many cases is

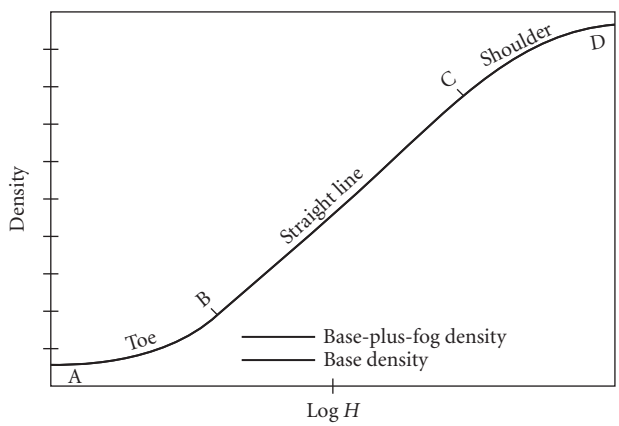

FIGURE 3 Typical D-log H curve for a negative photographic material. (*Reprinted courtesy Eastman Kodak Co. © Eastman Kodak Co.*)

Downloaded from Digital Engineering Library @ McGraw-Hill (www.accessengineeringlibrary.com)
Copyright © 2010 The McGraw-Hill Companies. All rights reserved.
Any use is subject to the Terms of Use as given at the website.

not an indication that the film is a linear responder in this region because, of course, both axes of the plot are logarithmic. It is worth noting here that the equation of the straight-line portion of this curve can be written

$$D = \gamma(\log H - \log C) \tag{8}$$

where γ is the slope of the straight-line portion and C is the exposure at the point where the extrapolated straight line cuts the exposure axis. Taking antilogarithms, Eq. (8) becomes

$$T = \left(\frac{H}{C}\right)^{-\gamma} \tag{8a}$$

If $\gamma = -1$, $T = (1/C)H$, and for this special case, the system becomes linear over the exposure range corresponding to the straight-line portion. A negative value of γ indicates a *positive* image.

A number of useful performance parameters for films are taken from their D-log H curves, as follows.

1. *Fog:* For most films, a certain number of grains will be reduced even though they have received no exposure at all, or insufficient exposure to form a latent image speck. The resulting density is called *fog*. Since it is not exposure-related, and since it tends to veil any information recorded in the toe, excessive fog is very undesirable. For many purposes, the fog density plus the density of the support are subtracted from the gross density to give the value of the net density resulting from the exposure. More complicated formulas for correcting the film's response for fog grains have been proposed, but are rarely used.
2. *Gamma:* Traditionally, the slope of the straight-line portion of the D-log H curve is called the "gamma." Gamma is a crude measure of the contrast with which the original object is reproduced; it would be a good measure of this contrast if the object were in fact recorded entirely on the straight-line portion of the response curve. However, for many purposes, notably pictorial photography, an appreciable part of the toe is used. This fact led Niederpruem, Nelson, and Yule to propose the use of an average gradient that included part of the toe as a measure of the contrast of the reproduction.[12] This quantity is called the *contrast index*. Since it includes part of the toe, contrast index is less than gamma. Since information is often recorded in the toe, it is convenient to generalize the meaning of γ to refer to the gradient anywhere along the D-log H curve, and this is done in this chapter. Note that in this case, the traditional gamma is the maximum value the gradient attains.
3. *Latitude:* Latitude can be defined as the log exposure range between the point in the toe and the point in the shoulder between which the gradient is equal to or greater than the minimum value required for acceptable recording. Clearly, the latitude of the film must be at least equal to the log exposure range of the object for proper recording. In many practical cases the film's latitude easily exceeds the required range. Note that the latitude is determined in part by the maximum density that the film can produce.
4. *Speed:* Speed is defined by the general expression

$$S = \frac{K}{H_{\text{ref}}} \tag{9}$$

where K is a proportionality factor and H_{ref} is the exposure required to produce some desired effect. Since the desired effect varies depending on the type of film and the application, H_{ref} also varies. Also, H_{ref} can be stated in either radiometric or photometric units. If H_{ref} is given in radiometric units, the proportionality factor K is set to unity, and the resulting values are termed "radiometric speeds." Although radiometric speeds are the fundamental speed values, they are rarely used in practice because, as previously noted, exposures are usually given in photometric units. In this case, the factor K takes on different values that depend not only on H_{ref}, but also on the characteristics of the exposure meter, which is standardized.[13] Varying the factor K allows a single meter to be used with

Downloaded from Digital Engineering Library @ McGraw-Hill (www.accessengineeringlibrary.com)
Copyright © 2010 The McGraw-Hill Companies. All rights reserved.
Any use is subject to the Terms of Use as given at the website.

all kinds of films and applications, which is a practical necessity. Thus, for example, the photometric speed (usually simply the "speed") of black-and-white pictorial films is evaluated from

$$S = \frac{0.8}{H_{0.1}} \tag{9a}$$

where $H_{0.1}$ is the exposure in lux-seconds required to produce a density of 0.1 above the densities of the base plus fog in a specified process. This density level has been shown empirically to be predictive of excellent tone reproduction quality in the print. Similarly, for color slide films

$$S = \frac{10}{H_m} \tag{10}$$

where H_m is the exposure to reach a specified position on the film's D-log H curve. Again, H_m was established empirically. The above two examples show how the two factors involved in determining a photometric or practical speed can vary. A number of other speeds have been defined and are described in the literature.[14]

Variation of Sensitometry with Processing

The rate of reduction of the exposed photographic grain depends on the characteristics of the grain itself, the formulation of the developer, and its temperature. In general, the reaction is allowed to continue until substantially all exposed grains have been reduced, and ended before fog becomes excessive. Many modern films are hardened and able to withstand processing temperatures up to, say, 40°C. Development times are often chosen on the basis of convenience and usually run in the order of 5 to 10 minutes in nonmachine processing. As development time and/or temperature are increased, the amount of density generated naturally increases. Thus for a given film a whole family of response curves can be produced, as shown in Fig. 4. As development time is lengthened, gamma and contrast index also increase. Typical behavior of these parameters is shown in the inset of Fig. 4.

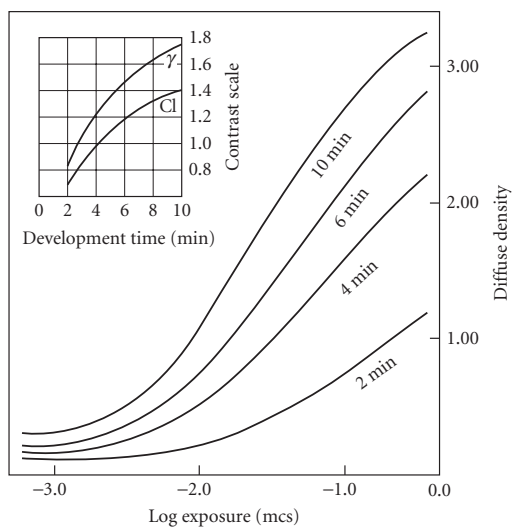

FIGURE 4 A family of characteristic curves for development times as shown, with corresponding plots of contrast index and gamma, mcs or the meter-candle second, as stated on p. 29.6, is the old term for lux-second or lxs. (*Reprinted courtesy Eastman Kodak Co. © Eastman Kodak Co.*)

Downloaded from Digital Engineering Library @ McGraw-Hill (www.accessengineeringlibrary.com)
Copyright © 2010 The McGraw-Hill Companies. All rights reserved.
Any use is subject to the Terms of Use as given at the website.

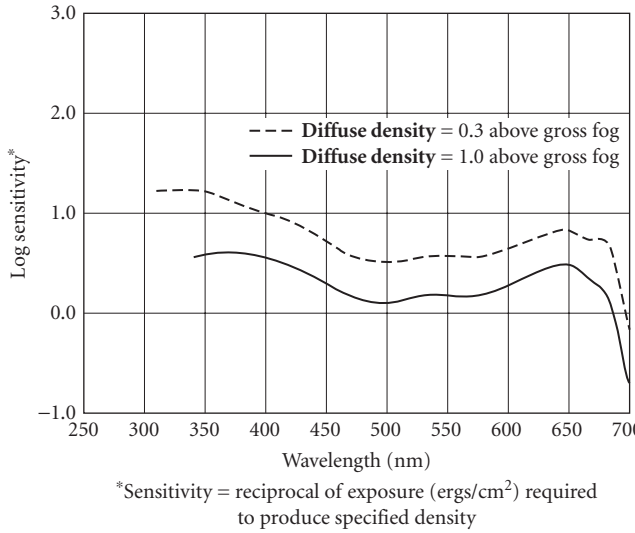

FIGURE 5 Spectral sensitivity curves for a modern negative material sensitized to about 690 nm. (*Reprinted courtesy Eastman Kodak Co. © Eastman Kodak Co.*)

29.8 SPECTRAL SENSITIVITY

The spectral absorption of the silver halide grain extends only to about 500 nm, and thus the inherent sensitivity of the grain is limited to regions shorter than that limit. However, it was discovered by Vogel in 1873 that sensitivity could be extended to longer wavelengths by dyeing the grains, and over the years the effective sensitivity range was extended into the infrared. Presently, materials are available usefully sensitized out to about 1.2 μm, but it should be noted that IR materials tend to have poor shelf life, and may require special handling. For our purposes, we may say that the sensitizing dye absorbs the incident energy in the required spectral region and transfers the energy to the grain in a manner that produces the required latent-image speck. The mechanisms are discussed in Ref. 3, chap. 10.

The spectral sensitivity of a photographic layer is usually specified by a family of curves showing log $(1/H_D)$ vs λ, where H_D is the exposure in ergs/cm^2 of wavelength λ required to produce some stated density. Spectral sensitivity values are thus radiometric speeds. Typical curves are shown in Fig. 5. In practical work, three broad classes of sensitization are recognized, which are called "color-blind" (or blue-sensitive), orthochromatic (additionally sensitized to green), and panchromatic (additionally sensitized to green and red). Most modern general-purpose materials are panchromatic.

In general, the shape of the spectral sensitivity curve follows that of the spectral absorption of the layer. It should also be noted that the gradient of the D-log H curve will be affected by the absorption of the layer. Gamma may therefore vary as a function of wavelength, and is generally somewhat lower in the blue and UV regions of the spectrum. This means that if the material is being used as a radiometer, it must be calibrated at the wavelength(s) of interest.

29.9 RECIPROCITY FAILURE

It was noted above that the exact response of a photographic layer may change due to exposure effects. Of these, the phenomenon of *reciprocity failure* is the most important in practical photography.

Downloaded from Digital Engineering Library @ McGraw-Hill (www.accessengineeringlibrary.com)
Copyright © 2010 The McGraw-Hill Companies. All rights reserved.
Any use is subject to the Terms of Use as given at the website.

By definition [Eq. (1)] exposure is simply the product of the irradiance and time, and nothing in this definition specifies the magnitude of either factor. However, the developed *density* resulting from a given calculated exposure is often found to depend on the *rate* at which the radiation is supplied, all other factors being held constant. Broadly speaking, exposure times of about 0.01 to 1.0 second are most efficient in producing density, the exact values depending on the film involved. Times much outside the above range tend to produce lower density for the same calculated exposure. The emulsion-maker has some ways of minimizing the effect, and usually attempts to optimize the response for the exposure times expected to be used with the material. Reciprocity failure is discussed in detail in Ref. 3, chap. 4, sec. II.

The loss of efficiency for short-time and correspondingly high-irradiance exposures is termed "high-intensity reciprocity failure," and that for long exposure times (low irradiances) is termed "low-intensity reciprocity failure." The Gurney-Mott mechanism explains both types of failure well. Note also that the names are misnomers; the terms should, of course, be high and low *irradiance*.

Only limited data are available, but the gradient of the D-log H curve tends to decrease as exposure times are shortened. An example is shown in data published by Hercher and Ruff.[15] Limited data also indicate that the speed loss due to high-intensity failure stabilizes for times shorter than about 10^{-5} second.[16] Essentially, the amount of reciprocity failure is independent of exposing wavelength.[17] This is to be expected.

Reciprocity failure may be a considerable problem for photographers working in specialized time domains, such as oscilloscope photography or astronomy. Astronomers have been able to devise user treatments for minimizing low-intensity failure.[18] For the practical photographer, reciprocity failure sometimes appears as a problem in color photography. If the RF of the three sensor layers differs, the resulting picture may be "out of balance," i.e., grays may reproduce as slightly tinted. This is very undesirable, and correction filter recommendations are published for some films for various exposure times.

29.10 DEVELOPMENT EFFECTS

Besides exposure effects the final density distribution in the developed image may be affected by "development effects" arising from chemical phenomena during development. Various names such as "border effect," "fringe effect," "Eberhard effect," etc., are applied to these phenomena; what we shall here term "edge effect" may be important in practice.

Consider a sheet of black-and-white film developing in a tray, and assume for purposes of discussion that there is no motion of the developer. Since developing agent must be oxidized as halide is reduced, and since the by-products of this reaction may themselves be development inhibitors, it can be seen that local variations of developer activity will be produced in the tray, with the activity decreasing as density increases. Agitation of the solution in the tray reduces the local variations, but usually does not eliminate them entirely, because it is the developer that has diffused into the gelatin matrix that is actually reacting. Now an "edge" is a boundary between high- and low-density areas, as shown in Fig. 6. Because of the local exhaustion and the diffusion phenomena, the variation of developer activity within the layer will be as shown by the dotted line in the figure. The result is that the developed density near the edge on the low-density side tends to decrease, and on the high-density side tends to increase, as also shown in the figure. In other words, the density distribution at the edge is changed; this actually occurs to some degree in much practical work and has interesting consequences, as will be discussed below.

The local exhaustion of the developer may also be important in color films where development in one layer (see below) may affect the response of an adjacent layer. In color photography, the phenomenon is called "interimage effect."

29.11 COLOR PHOTOGRAPHY

Color photography has been extensively reviewed by Kapecki and Rodgers.[19] With one exception at the time of writing, all commercially available color films employ subtractive color reproduction. The exception is an instant film for color slides marketed by Polaroid Corporation, which employs

Downloaded from Digital Engineering Library @ McGraw-Hill (www.accessengineeringlibrary.com)
Copyright © 2010 The McGraw-Hill Companies. All rights reserved.
Any use is subject to the Terms of Use as given at the website.

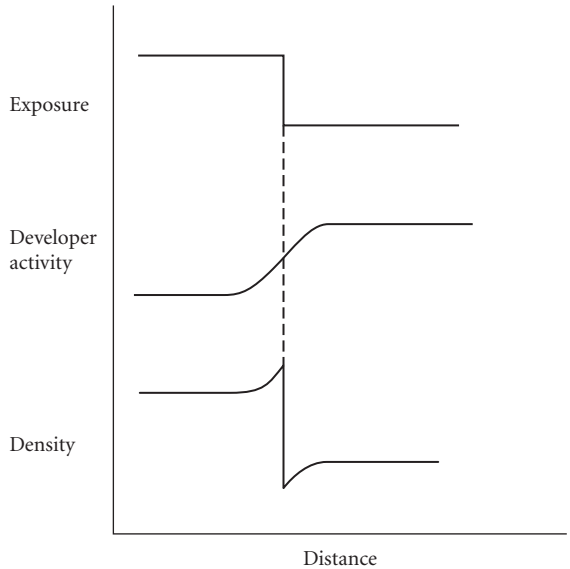

FIGURE 6 Distributions of developer activity and density resulting from a step-function input in the presence of edge effect.

additive color. The mechanism involves a reseau of very fine red, green, and blue stripes, which provide the color separation during the taking of the photograph, and also the color when the (reversed) image is projected.[20]

The basic structure of most other color films is similar to that shown in Fig. 7. The incoming light first encounters a nonspectrally-sensitized emulsion layer, which records the blue-light elements of the scene. The next layer is a yellow, or minus-blue filter, the purpose of which is to prevent any blue light from reaching the other two emulsion layers. This yellow filter is usually composed of "Carey Lea," or colloidal silver dispersed in gelatin. Such sols are yellow. The reason for using Carey Lea silver is that all metallic silver is removed from the film during processing anyway, and the necessary removal of the filter layer is thus accomplished automatically.

Moving downward in the stack, the next layer is an ortho-sensitized emulsion. Since any blue light has been blocked by the yellow filter, this layer records the green-light elements of the scene. The final layer in the stack is sensitized to red light but not to green light and this layer serves to record the red elements of the scene. Modern films usually contain many more than the four layers indicated here, but the operating principles of the film can be discussed in terms of such a "tripack." In accordance with the principles of subtractive color reproduction, the images in the three separation

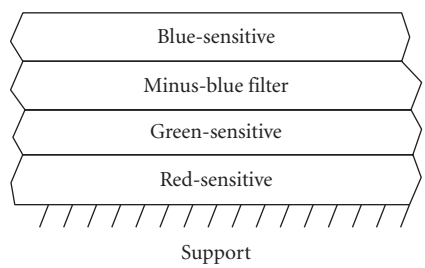

FIGURE 7 Schematic tripack structure of a color film.

Downloaded from Digital Engineering Library @ McGraw-Hill (www.accessengineeringlibrary.com)
Copyright © 2010 The McGraw-Hill Companies. All rights reserved.
Any use is subject to the Terms of Use as given at the website.

records are then converted to yellow, magenta, and cyan dyes, respectively, and the final image is composed of these dyes, without the developed silver, which is either removed chemically or left behind, depending on the exact material.

Within this broad framework, films can be separated into two classes: chromogenic and nonchromogenic. In the former class, the dyes are not coated in the film, but are formed during the processing by a reaction called "coupling." In coupling, the by-products of the halide reduction reaction serve as components for a second reaction in which dye is formed; the amount of dye thus increases as density increases. The components of the dye-forming reaction (i.e., other than the development by-products) may be present in the developing solution (Eastman Kodak Co., "Kodachrome") or, more generally, coated within the various layers (Kodacolor, Polaroid "One Film," Agfachrome, Fujicolor, etc.). After the required dyes are formed, the developed silver is removed by a chemical process termed "bleaching."

The advantage of incorporating the couplers in the various layers of the tripack is simpler processing, but because of the additional material in the layers, such films tend to be not as sharp as the nonincorporated-coupler types. Chromogenic color films are available both as slide materials, in which the film undergoes a reversal process,[21] and as color negative—color print materials in which a dye negative is formed and then printed onto a color paper whose structure is fundamentally similar to that of the films.

The principal example of the nonchromogenic film is the Polaroid Instant Color Film. In this film the yellow, magenta, and cyan dyes are actually coated in the structure, along with the blue, green, and red-sensitive emulsions. When development takes place in a given layer, the corresponding dye is immobilized. The dye that has *not* been immobilized in the three layers migrates to a "receiver" layer, where it is mordanted. Since the amount of dye that migrates *decreases* as the original density *increases*, the result is a positive color image formed in the receiver. The material has been described in more detail in a paper by Land,[22] and also in chap. 6 of Ref. 4.

The image in a color film thus essentially consists of three superimposed dye images. Typical spectrophotometric curves for dyes formed by coupling reactions are shown in Fig. 8. The density of any one of these dye layers taken by itself is known as an *analytical* density. Note, however, that all the dyes show some "unwanted" absorption—that is, absorption in spectral regions other than the specific region that the dye is supposed to control. Thus the total density of the layer at any wavelength is the sum of the contributions of all three dyes; this type of density is known as "integral density." The integral density curve is also shown in Fig. 8.

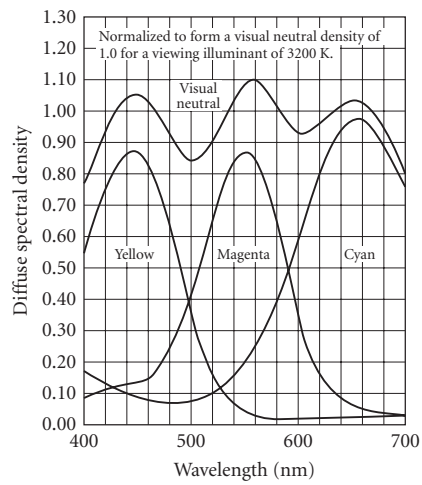

FIGURE 8 Spectral dye density curves for a color film. (*Reprinted courtesy Eastman Kodak Co. © Eastman Kodak Co.*)

Downloaded from Digital Engineering Library @ McGraw-Hill (www.accessengineeringlibrary.com)
Copyright © 2010 The McGraw-Hill Companies. All rights reserved.
Any use is subject to the Terms of Use as given at the website.

The reproduction of color by photographic systems has been discussed by Hunt[23] and many others.[24] In general, exact colorimetric reproduction is not achieved, but for most purposes the reproduction of the hues and luminances in the original scene is satisfactory. Evans,[25] in fact, observes that under the right conditions the "magnitude of the reproduction errors that can be tolerated is astonishing." One aspect that is critical for many workers, especially expert photographers, is the ability of the system to produce good "balance," i.e., to reproduce a neutral as a neutral. This requirement is so important that one of the types of density that is measured for dye layers is the *equivalent neutral density* (END) which is defined as the visual neutral density that a dye layer would produce if combined with the correct amounts of the other two dyes (whatever those correct amounts may be). When the ENDs of the three layers are equal, the system is in balance, and color-film sensitometry is therefore often done in terms of ENDs. Further discussion of color sensitometry and densitometry may be found in Ref. 3, chap. 18.

29.12 MICRODENSITOMETERS

As indicated above, a microdensitometer is a densitometer designed to measure the density of a small area. The sampling apertures are typically slits which may be as narrow as 1 to 2 μm in nominal width. The sample is scanned over the aperture, creating a record of density as a function of position on the sample surface, i.e., distance.

In practical instruments, the small sampling aperture dimensions are achieved by projecting an enlarged image of the film onto a physical aperture. The optical system produces some effects not encountered in macrodensitometers, as follows:

1. In general, microdensitometers measure projection, or semispecular, density. As already noted, projection density is higher than diffuse density for silver layers, and the exact value of the effective Callier coefficient Q' depends in part on the numerical aperture of the optical system. Thus two microdensitometers fitted with optics of different NAs may give different density values for the same sample. Furthermore, macrodensity data are usually in terms of diffuse density, so that data from the microdensitometer should be corrected if intercomparisons are to be made. The effective Callier coefficient for the specific optics-sample combination is easily determined by measuring suitable areas of sample both in the microdensitometer and a macrodensitometer, and taking the ratios of the values.
2. The presence of stray light in the system tends to lower the measured density. This problem is especially troublesome in microdensitometry because of the types of images that are often encountered. Thus, for example, when an interface between clear and dense areas—that is, an edge—is scanned, stray light will distort the record in the manner shown in Fig. 9. If the image is that of a star or spectroscopic line, this behavior results in an artifically low density reading. It is very important to control stray light as completely as possible in microdensitometry.

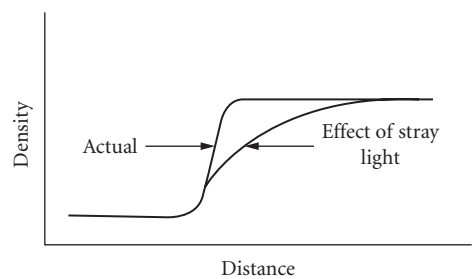

FIGURE 9 Effect of stray light in the microdensitometer on the apparent density distribution at an edge.

Downloaded from Digital Engineering Library @ McGraw-Hill (www.accessengineeringlibrary.com)
Copyright © 2010 The McGraw-Hill Companies. All rights reserved.
Any use is subject to the Terms of Use as given at the website.

3. One feature of the usual microdensitometer optical system, installed for control of stray light, is the "preaperture," a field stop that limits the area of the sample that is illuminated. Because of this preaperture, and the optical system, a normal microdensitometer is a partially coherent system. This means that the instrument may respond to path-length differences in the sample as well as to density differences. This is undesirable since in practice it is the density differences that carry the information. Partial coherence in microdensitometers has been studied by Thompson and by Swing among others, and the results are summarized by Dainty and Shaw.[26] It has been shown that the coherence effects can be minimized by satisfying two conditions. In the first condition, the width W of the preslit

$$W \geq \frac{4\lambda}{NA_{\text{in}}} \tag{11a}$$

The second condition is

$$\frac{NA_{\text{in}}}{NA_{\text{eff}}} = 1 + \frac{\nu_s}{\nu_o} \tag{11b}$$

where λ = the wavelength of the light
NA_{in} = numerical aperture of the influx optics
NA_{eff} = numerical aperture of the efflux optics
ν_s = maximum spatial frequency in the sample
ν_o = spatial frequency cutoff of the scanning objective

If, for example $\nu_o = 3\nu_s$, then $NA_{\text{in}}/NA_{\text{eff}} \geq 1.3$. A microdensitometer arranged to minimize coherence problems is called a *linear* microdensitometer. Note that the two conditions above conflict with conditions commonly adopted to control stray light.

29.13 PERFORMANCE OF PHOTOGRAPHIC SYSTEMS

The following discussion of performance is limited to those aspects which are properties of the system, and excludes such aspects as the skill of the photographer, etc. Of those aspects, which we may term "technical" quality parameters, the most important is *tone reproduction*. The subject is divided into two areas: subjective tone reproduction and objective tone reproduction. Subjective tone reproduction is concerned with the relation between the brightness sensations produced in the observer's mind when the scene is viewed and when the picture is viewed. Since the sensation of brightness depends markedly on the viewing conditions and the observer's state of adaptation, the subjective tone reproduction of a given picture is not constant, and this aspect of the general subject is not often measured in the photographic laboratory. It is discussed by Kowalski.[27] Objective tone reproduction is concerned with the reproduction of the luminance and luminance differences of the scene as luminances in the final output. Tone reproduction studies apply equally well to projected images, prints, transparencies, and video images, but a negative-print system is usually assumed for discussion. It is easy to show that the log luminance of a print area, $\log L_p = C - D_p$, where C is a constant determined by the illuminance on the print and D_p is the density of the print area. Thus tone reproduction curves are usually plotted in the form of the print density versus the log luminance of the corresponding scene element (Fig. 10). Although both the scene luminances and the print densities are fixed quantities, the viewer's reaction still depends on the illumination level at which the picture is seen.

It has been shown empirically that for paper prints viewed under typical "room lighting conditions," the preferred tone reproduction curve is the solid line in Fig. 10. Perfect objective tone reproduction, defined as the case where $\Delta D_p = -\Delta \log L_{sc}$ for all scene luminance levels, would be

Downloaded from Digital Engineering Library @ McGraw-Hill (www.accessengineeringlibrary.com)
Copyright © 2010 The McGraw-Hill Companies. All rights reserved.
Any use is subject to the Terms of Use as given at the website.

PHOTOGRAPHIC FILMS

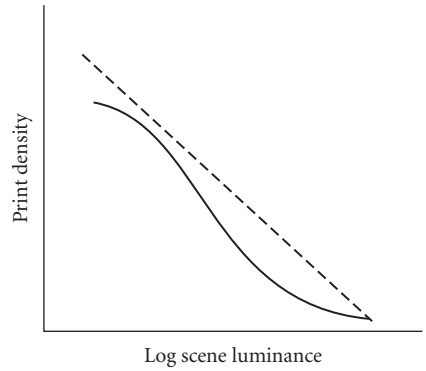

FIGURE 10 Preferred tone reproduction for viewing under typical room lighting conditions.

the dotted line in the figure. Thus under typical room lighting conditions viewers prefer a reproduction that has somewhat more contrast and less density than the "perfect" result. This preference will, however, change with illumination and stray light levels.

The exact shape of the tone reproduction curve obtained with a given system depends on the shape of the negative and positive D-log H curves, and also on the stray-light characteristic of the camera system. (Excessive stray light in the camera can be very deleterious to tone reproduction quality.) Using a graphic method devised by Jones and described by Nelson and others,[28] the effect of the D-log H curves and the stray light on the tone reproduction can be studied.

29.14 IMAGE STRUCTURE

The other two technical quality parameters of a photographic system are its sharpness and graininess, to use the most familiar terms for these properties. These properties are often lumped together under the general term "image structure." Actually, in photoscience the term sharp*ness* and grain*iness* are reserved for the subjective aspects of the phemomena, and measurement of these properties requires psychometric testing. Since such testing is expensive and time-consuming, objective correlates of both properties have been defined, and methods for measurement have been established. The objective correlate of sharpness is termed *acutance*, and of graininess is termed *granularity*. Image structure data for various kinds of materials are given in Table 1, along with speed and contrast values.

29.15 ACUTANCE

The original proposal for measuring acutance was made by Higgins and Jones[29] in 1952. It involved calculating a value from a microdensitometer trace of a test edge. However, the visual processes that occur when an observer views an edge are complex, and the straightforward calculation proposed by Higgins and Jones fails to predict the sensation of sharpness produced by some edge distributions. At about the same time, the optical transfer function (OTF) and related concepts began to be widely used in optics, and these were soon applied to photographic materials also.

The concepts of the point and line spread functions are essentially identical in optics and photoscience; in the photographic layer the smearing of the point (or line) input is caused by diffraction around the grains, refraction through them, and reflection from them. These phenomena are usually

Downloaded from Digital Engineering Library @ McGraw-Hill (www.accessengineeringlibrary.com)
Copyright © 2010 The McGraw-Hill Companies. All rights reserved.
Any use is subject to the Terms of Use as given at the website.

TABLE 1 Performance Data for Types of Materials[a]

Type	SPD[b]	γ	Gran.[c]	ν_{50}[d]
B&W microfilm	80	3.0	6	>200
B&W very slow camera neg.	25	0.5–3.5	5–7	80–145
B&W slow camera neg.	100	0.5–1.1	8–9	65–120
B&W fast camera neg.	400	0.5–1.0	10–14	50–100
B&W very fast camera neg.	1600–3200	0.5–1.0	18	70
Color neg. very slow	25–50	0.65	4–5	40–60
Color neg. slow	100–160	0.60–0.80	4–6	30–70
Color neg. fast	400	0.65–0.80	5–7	25–40
Color neg. very fast	1000–1600	0.80	8–11	25–35
Color rev. slide very slow	25–50	1.8–2.3	9–10	30–40
Color rev. slide slow	100	2.0–3.0	10–13	25–30
Color rev. slide fast	400	2.0–2.4	15–20	20
Color rev. slide very fast	800–1600	2.2–2.8	22–28	16–20
Instant print films[e]		–1.7[f]	NA	3–4
—Black and white	3000	–1.6	NA	2.5
—Color	100			

[a]Data are as of early 1993 and were obtained from publications of the manufacturers listed in Sec. 29.21. They are presented as published. Note that products are frequently changed or improved.

[b]Speeds are calculated in different ways for various classes of product. The values given are suitable for use with standard exposure meters.

[c]Values represent 1000× the standard deviation of the diffuse density, measured at an average density of 1.0 using a 48-μm circular aperture. The exact granularity of a print depends on the characteristics of the print material and the printer as well as the granularity of the negative.

[d]Values show the spatial frequency at which the modulation transfer function is 50 percent.

[e]MTF values apply to the final print.

[f]Negative sign arises from the definition of gamma for the case of a positive image.

lumped together and termed "scattering," and have been treated by Gasper and dePalma.[30] Likewise, the concept of the optical transfer function, or the Fourier transform of the LSF, is basically the same in optics and photography. However, three important differences should be noted for the photographic case. (1) The emulsion is isotropic, so that the PSF and LSF are always symmetrical, and the complex OTF reduces to the modulation transfer function (MTF) only. (2) Unlike lenses, photographic layers are stationary, but are generally nonlinear. Therefore, all data and calculations must be in terms of *exposure* or allied quantities. When the calculations are complete, the results are converted to density via the D-log H curve. (3) The presence of edge effects tends to raise the MTF curve, so that for low frequencies the measured response values are often found to be greater than 100 percent. The subject is treated in detail by Dainty and Shaw.[31] Typical MTF curves for a film, showing the overshoot, are given in Fig. 11. Data for MTF curves of various types of films are also given in Table 1. The value given shows the spatial frequency for which the transfer factor drops to 50 percent.

The chain relating the MTF curve to image sharpness is the same as in optics: a high MTF curve transforms to a narrow spread function, and this in turn indicates an abrupt transition of exposure—and therefore density—across the edge. Thus MTF response values greater than unity, although mathematically anomalous, indicate improved image sharpness, and this is found to be the case in practice. As a matter of fact, edge effects are often introduced deliberately to improve sharpness. This is done either by adding suitable compounds to the coating itself, or by adjusting the developer formulation. The process is similar to the electronic "crispening" often used in television.

An index of sharpness can be computed from the MTF data by a procedure first suggested by Crane and later modified by Gendron.[32] These workers were interested mainly in films, but they recognized that the film is one component of a system; e.g., a color slide system involves a camera lens, the film (and process), a projector lens, the screen, and the observer's eye. The MTF of the system is then the cascaded MTFs of these components. Gendron suggested that the area under the cascaded MTF be taken as the stimulus that produced the sensation of sharpness. A formula was proposed

Downloaded from Digital Engineering Library @ McGraw-Hill (www.accessengineeringlibrary.com)
Copyright © 2010 The McGraw-Hill Companies. All rights reserved.
Any use is subject to the Terms of Use as given at the website.

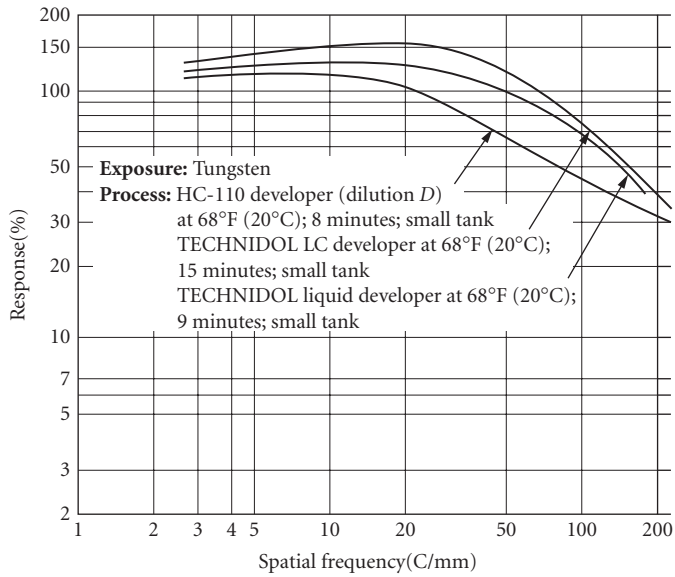

FIGURE 11 Modulation transfer functions of Kodak Technical Pan Film for three conditions of development. Note that the response at low frequencies exceeds 100 percent. (*Reprinted courtesy Eastman Kodak Co. © Eastman Kodak Co.*)

that produced a sharpness index scaled to 100. This index, now called CMT-Acutance (to distinguish it from the original Higgins-Jones acutance) has been found to correlate well with subjective data, and is used in the industry. Note that the treatment above has been simplified for the sake of brevity; details are available in Gendron's paper.

29.16 GRAININESS

The granular nature of the photographic image is one of its most significant characteristics. It may appear to the observer as an unpleasant roughness in what should be uniform areas, but it may also interfere with extracting information from the image. In the former case it is an aesthetic problem; in the latter case the structure is equivalent to noise in a communications channel. In either case it is desirable to measure the phenomenon objectively and in engineering terms.

The procedure now used for making these objective measurements was proposed by Selwyn in 1935.[33] He postulated that if the density of a uniformly exposed and processed layer were measured at many places using a suitable sampling aperture, the population of density values so obtained would be approximately gaussianly distributed around the mean. This being so, the variability for a given mean density is completely described by the standard deviation of the values. This quantity is termed the *rms-granularity*, $\sigma(D)$, and has indeed been shown to correlate with the subjective graininess.[34] It might be noted that calculating the standard deviation of the density is mathematically improper, since the underlying transmittance values are being multiplied. To avoid this problem the rms-granularity is formally defined by

$$\sigma(D) = \frac{0.434\sigma(T)}{\bar{T}} \tag{12}$$

where T is transmittance. However, it can be shown that when $\sigma(T)$ is small compared to $\bar{T}$, the error involved in calculating directly in density is small, and this is often done in practice.

Downloaded from Digital Engineering Library @ McGraw-Hill (www.accessengineeringlibrary.com)
Copyright © 2010 The McGraw-Hill Companies. All rights reserved.
Any use is subject to the Terms of Use as given at the website.

Selwyn also showed that the measured value of $\sigma(D)$ depended upon A, the area of the sampling aperture. The product $\sigma(D)A^{1/2}$ may be termed the *Selwyn coefficient* $\mathcal{G}$; for black-and-white films exposed to light, Selwyn showed that it should be constant, and this relation is called "Selwyn's law." Thus $\sigma(D)A^{1/2}$ is a measure of sample graininess no matter what the size of the sampling aperture. Unfortunately, the Selwyn coefficient does not remain constant with changes of aperture size for very important classes of samples. Selwyn's law may fail for prints and enlargements, black-and-white or color, for many color materials even if not enlarged, and also for radiographs, especially screened radiographs. For such materials $\sigma(D)$ still increases as A decreases, but not at a rate sufficient to keep the Selwyn coefficient constant, and it (the coefficient) is therefore not useful as an objective measure of graininess.

Stultz and Zweig[35] found that they obtained good correlation between $\sigma(D)$ and the sensation of graininess when the sampling aperture was selected in accordance with the rule

$$d(\mu)\cdot M_\theta \approx 515 \tag{13}$$

where $d(\mu)$ is the diameter of the sampling aperture in μm, and M_θ is the angular magnification[36] at which the photograph is seen by the viewer. M_θ is readily calculated from the relation

$$M_\theta = \frac{m}{4V} \tag{13a}$$

where m is the ordinary lateral magnification between the film image and the image presented to the viewer, and V is the viewing distance in meters.

An American standard[37] exists for the measurement of rms-granularity. This standard specifies that samples be scanned with a 48-μm-diameter aperture; for such an aperture, rms-granularity values for commercial films range from about 0.003 to 0.050 at an average density of 1.0. In practice, these values are often multiplied ×1000 to eliminate the decimals. It is worth noting that, experimentally, the measurement of rms-granularity is subject to many sources of error, such as sample artifacts. The standard discusses sources of error and procedures for minimizing them, and is recommended reading for those who must measure granularity.

While in practice rms-granularity serves well as an objective correlate of graininess, the situation is complicated by the fact that there are two broadly different types of granular pattern. Silver grains are small, opaque, and in nearly all cases are situated randomly and independently in the coating. The granular structure in an enlargement, however, is composed of clusters of print-stock grains that reproduce the exposure pattern coming from the enlarged negative grains. This type of granular pattern tends to be large and soft-edged compared to the pattern arising from the primary grains. The patterns found in such samples as color films and screened radiographs are generally similar to those found in enlargements. Microdensitometer traces of these two structures are illustrated in Fig. 12. A little thought will show that the two patterns shown in the figure might have the same mean and standard deviation, and yet the two patterns look entirely different. When different types of patterns are involved, the rms-granularity above is not a sufficient descriptor. The work by Bartleson which showed the correlation between graininess and rms-granularity was done with color negative films having similar granular structures.

As discussed by Dainty and Shaw,[38] further objective analysis of granular patterns may be carried out in terms of the *autocorrelation function*:

$$\phi(\tau) = \lim_{x\to\infty}\frac{1}{2x}\int_{-x}^{+x}\delta(x)\delta(x+\tau)dx \tag{14}$$

where $\delta(x) = D_x - \bar{D}$

Dx = the density reading at point x on the sample

$\bar{D}$ = mean density

$\delta(x+\tau) = D_{x+\tau} - \bar{D}$

τ = a small increment of distance

Note carefully that for the sake of simplicity it has been assumed that the sample is scanned by a very long, narrow slit, so that the autocorrelation function reduces to a one-dimensional function.

Downloaded from Digital Engineering Library @ McGraw-Hill (www.accessengineeringlibrary.com)
Copyright © 2010 The McGraw-Hill Companies. All rights reserved.
Any use is subject to the Terms of Use as given at the website.

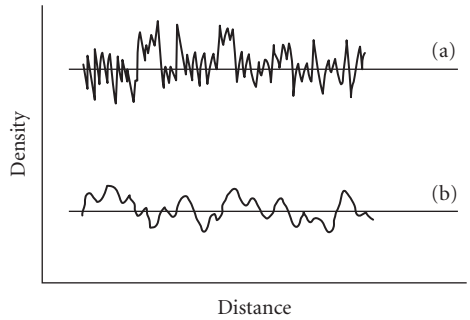

FIGURE 12 Microdensitometer traces of (*a*) primary silver grains and (*b*) granular structure of a print.

If the sample is scanned by a small circular aperture it will be two-dimensional. The use of a slit is common in practice. For the case where $\tau = 0$, we have

$$\phi(0) = \lim_{x\to\infty} \frac{1}{2x} \int_{-x}^{+x} [\delta(x)]^2 \, dx = \sigma^2 \tag{15}$$

Let $\phi(\tau)$ be calculated for several different values of τ, including values smaller than the slit width. Since when $\tau < w$ the slit will contain some of the same grains at points x and $x + \tau$, correlation is observed. If there is no spatial correlation in the actual sample, $\phi(\tau) \to 0$ for $\tau > w$. Positive values of $\phi(\tau)$ for $\tau > w$ are an indication of spatial correlation in the sample; that is, large-scale grain.

In practice, it is convenient to carry out the analysis of large-scale patterns in the spatial frequency domain. The Wiener-Khintchin theorem states that what is called the "Wiener spectrum" or *power spectrum of the granularity* distribution is the Fourier transform of the autocorrelation function; that is,

$$\mathrm{WS}(\nu) = \int_{-\infty}^{\infty} \phi(\tau) e^{i2\pi\nu\tau} \, d\tau \tag{16}$$

and also

$$\phi(\tau) = \int_{-\infty}^{\infty} \mathrm{WS}(\nu) e^{-i2\pi\nu\tau} \, d\nu \tag{16a}$$

where ν = spatial frequency.

In practice, an approximation of the Wiener spectrum is usually obtained by a direct Fourier transform of the granularity trace itself according to the expression

$$\mathrm{WS}(\nu) = \lim_{x\to\infty} \frac{1}{2x} \overline{\left| \int_{-x}^{x} \delta(x) e^{i2\pi\nu x} dx \right|^2} \tag{17}$$

where $\delta(x)$ has the same meaning as before, and the horizontal bar indicates that the average value of several different runs should be taken in order to provide a reasonable value for the approximation.

Returning to the definition of the autocorrelation function [Eq. (14)] it can be seen that the measured values of $\delta(x)$ and $\delta(x + \tau)$ are each actually the true values convolved with the slit response. By the convolution theorem of Fourier transforms, this means that in frequency space

$$\mathrm{WS}(\nu)_{\text{measured}} = \mathrm{WS}(\nu)_{\text{true}} \, x \, T(\nu)^2 \tag{18}$$

Downloaded from Digital Engineering Library @ McGraw-Hill (www.accessengineeringlibrary.com)
Copyright © 2010 The McGraw-Hill Companies. All rights reserved.
Any use is subject to the Terms of Use as given at the website.

where $T(\nu)$ is the modulation transfer factor of the measuring system at spatial frequency ν. If $T(\nu)^2$ is divided out of $\mathrm{WS}(\nu)_{\mathrm{measured}}$ the underlying net value $\mathrm{WS}(\nu)$ is obtained. When this is done for black-and-white film samples exposed to light, the underlying spectrum is found to be flat. For the kinds of samples for which Selwyn's law fails, on the other hand, the net Wiener spectrum is found to contain excess low-frequency power and lack high frequencies. Finally, by the properties of Fourier transforms, the area under the Wiener spectrum curve is the zero-value of the autocorrelation function. But by Eq. (15) this zero-value equals σ^2 for the sample, so that the area under the WS curve gives the rms-granularity of the sample. This can also be seen intuitively, since the value of the WS at special frequency ν is simply the noise power of σ^2 in a spatial frequency band $\nu \pm \Delta\nu/2$.

Doerner[39] has shown that the rms-granularity of a negative can be tracked through a printer system in terms of the Wiener spectrum of the negative and the modulation transfer function of the printer system (which includes the MTF of the print stock itself). Doerner's expression is

$$\mathrm{WS}(\nu)_p = \mathrm{WS}(\nu)_n \gamma_p^2 A(\nu)^2_{\mathrm{syst}} + \mathrm{WS}(\nu)_{\mathrm{ps}} \tag{19}$$

where n and p indicate negative and print respectively, "ps" the print stock itself, and the other symbols have their previous meanings. The granularity/graininess of a print thus depends on the contrast of the print stock and the spatial frequency response of the printer system as well as on the graininess of the negative.

29.17 SHARPNESS AND GRAININESS CONSIDERED TOGETHER

In the foregoing discussion, we have considered the sharpness and graininess aspects of the picture separately. But real photographs frequently suffer from less-than-optimum sharpness and graininess *both*. Bartleson[40] has studied the subjective quality of such photographs. He concluded that quality was not a linear combination of sharpness and graininess. Instead, ". . . quality tends to be determined primarily by the poorer of the two attributes. . . . If graininess is high, the print will likely be low in quality regardless of how sharp it may be or, conversely, if sharpness is low, so also will quality be low regardless of how grainy the print appears. . . ."

Bartleson's results are of interest in assessing the quality of electronic images, since, at least at the time of writing, such images exhibit low graininess, but also low sharpness. On the basis of Bartleson's work, such images would be judged to be of low subjective quality. In a comparison of electronic and film imagery published in 1990, Ikenoue and Tabei[41] rated the quality of the former as poor because of the sharpness level.

29.18 SIGNAL-TO-NOISE RATIO AND DETECTIVE QUANTUM EFFICIENCY

Since the information in a photograph is normally carried by the density variation, we may usefully define the output signal-to-noise ratio of the photography by

$$\mathrm{S/N}_{\mathrm{out}} = \frac{\Delta\bar{D}}{\sigma} = \frac{\gamma}{\sigma} \cdot \Delta \log H \tag{20}$$

where $\Delta\bar{D}$ is the mean density difference between an element to be detected and its surround, and σ is the rms-granularity of the surround. By Selwyn's law, $\sigma(D)$ varies as the area of the sampling

Downloaded from Digital Engineering Library @ McGraw-Hill (www.accessengineeringlibrary.com)
Copyright © 2010 The McGraw-Hill Companies. All rights reserved.
Any use is subject to the Terms of Use as given at the website.

aperture changes; it is convenient here to take the sampling aperture area A as equal to the area of the image element. Furthermore, for ΔH sufficiently small we may write

$$S/N_{out} = 0.434 \frac{\gamma}{\sigma} \cdot \frac{\Delta H}{H} \tag{21}$$

Note that γ/σ is a property of the film; it is termed the *detectivity*. $\Delta H/H$, on the other hand, is a property of the object; in fact, it is the object contrast. Practical tests have shown that S/N_{out} should be 4 to 5 if the element is to be detected against its surround, and 8 to 10 if it is to be recognized.[42]

In 1946, Albert Rose of RCA published a paper[43] in which he discussed the performances of the TV pickup tube, the photographic layer, and the human eye on a unified basis. His approach was to compare their performances with that of an "ideal device," that is, a radiation detector whose performance was limited only by the quantum nature of the incoming radiation. Such a perfect detector would report the arrival of every incoming quantum, and add no noise to the signal.

In 1958, R. Clark Jones of Polaroid expanded Rose's work with specific application to photographic layers.[44] Jones proposed the term *detective quantum efficiency* (DQE) for Rose's performance indicator, and defined it by the expression

$$DQE = \left[\frac{S/N_{out}}{S/N_{ideal}}\right]^2 = \left[\frac{S/N_{out}}{S/N_{max}}\right]^2 = \left[\frac{S/N_{out}}{S/N_{in}}\right]^2 \tag{22}$$

where S/N_{out} is the signal-to-noise ratio produced by the actual device, and S/N ideal is the ratio that would be produced by the ideal device, given the same input. By the definition of the ideal device, $S/N_{ideal} = S/N_{max} = S/N_{in}$, where S/N_{in} is the signal-to-noise ratio in the input, and is due to the quantum nature of the input. The ratio is squared to make the DQE compatible with various other concepts.

It is easy to derive an expression for the S/N ratio of the input; when this is combined with Eq. (21) the result is

$$DQE = \left[\frac{0.434\gamma}{\mathcal{G}}\right]^2 \cdot \frac{1}{q} \tag{23}$$

where $\mathcal{G}$ is the Selwyn coefficient and q is the average exposure received by the image in *quanta per unit area*. Since $(1/q)$ is the radiometric speed of the film, it can be seen that the DQE is a performance parameter that combines the gain (gamma), noise, and speed of the layer. As written, the DQE does not involve the sharpness aspect, but this can be included also.[45]

Since Eq. (23) involves standard photographic parameters, it is readily evaluated for a given material. When this is done, it is found that the DQE of typical materials is on the order of 1 to 3 percent, peaking sharply at low densities in the case of black-and-white films. Note that DQE can be calculated for any sensor for which S/N_{out} can be derived. It is interesting to compare the 1 to 3 percent values given above with those of other sensors. Thus, for example, Jones gives a value of 1 percent for the human eye, and 6 percent for an image orthicon tube. On the other hand, a suitable photographic layer recording electrons may approach 100 percent DQE, and a value of 30 percent has been reported for a screened x-ray film.[46] DQE has also served as a useful approach to considering silver halide mechanisms; see, for example, a paper by Bird, Jones, and Ames that appeared in *Applied Optics* in 1969.[47]

Another figure of merit allied to DQE is the *noise equivalent quanta* (NEQ) which is defined as the number of quanta that a perfect detector would need to produce a record having the same S/N ratio as the system under consideration. It can be shown that

$$q' = DQE \times q \tag{24}$$

where q is again the number of quanta/unit area used by the real system, and q' the NEQ of a unit area of image.

Downloaded from Digital Engineering Library @ McGraw-Hill (www.accessengineeringlibrary.com)
Copyright © 2010 The McGraw-Hill Companies. All rights reserved.
Any use is subject to the Terms of Use as given at the website.

29.19 RESOLVING POWER

The basic procedure used to measure photographic resolving power follows that used in optics. An American Standard exists.[48] The standard provides for a suitable test object to be reduced optically onto the material to be tested. (Strictly speaking, the test thus determines the resolution of the lens-film combination, but the resolution capability of the lenses specified is high compared to that of the film.) The developed image is then studied in a microscope to determine the highest spatial frequency in which the observer is "reasonably confident" that the structure of the test pattern can still be detected. Thus, as in optics, the "last resolved" image is a threshold image. However, unlike the optical case, the limit is set not only by the progressive decrease in image modulation as spatial frequency increases, but also by the granular nature of the image.

If an exposure series of the test pattern is made, it is found that the spatial frequency of the limiting pattern goes through a maximum. It is customary to report the spatial frequency limit for the optimum exposure as the resolving power of the film.

Photographic resolving power is now not much measured, but it retains some interest as an example of a signal-to-noise ratio phenomenon. Consider the modulation in the various triplet images in the pattern. By definition,

$$M = \frac{H_{\max} - H_{\min}}{H_{\max} + H_{\min}} = \frac{\Delta H}{2\bar{H}} \tag{25}$$

and from Eq. (21),

$$\Delta D = 0.868\,\gamma M \tag{26}$$

so that ΔD within the pattern varies as the modulation, which in turn decreases as the spatial frequency increases. Furthermore, the area of each of the triplets in the pattern (assuming the ISO pattern configuration) $= 2.5^2\lambda^2 = 2.5^2/\nu^2$. Assuming that Selwyn's law holds, it follows that $\sigma = \mathcal{G}/A^{1/2} = 0.4\,\mathcal{G}\nu = C\nu$, where we have lumped the constants. As the spatial frequency increases, the S/N of the triplet decreases because ΔD decreases and the effective rms-granularity increases. The resolving power limit comes at the spatial frequency where the S/N ratio drops to the limit required for resolution. Such a system has been analyzed by Schade.[49]

29.20 INFORMATION CAPACITY

The information capacity, or number of bits per unit area that can be stored on a photographic layer, depends on the size of the point spread function, which determines the smallest element that can be recorded, and on the granularity, which determines the number of gray levels that can be reliably distinguished. The exact capacity level for a given material depends on the acceptable error rate; for one set of fairly stringent conditions, Altman and Zweig[50] reported levels up to 160×10^6 bits/cm^2. Jones[51] has published an expression giving the information capacity of films as

$$IC = \frac{1}{2}\int\int_0^\infty \log_2\left(1 + \frac{S(\nu_x, \nu_y)}{N(\nu_x, \nu_y)}\right) d\nu_x\, d\nu_y \tag{27}$$

where S and N are the spectral distributions of power in the system's signal and noise. For a given spatial frequency, the signal power is given by

$$S = \mathrm{WS}_i(\nu)\mathrm{MTF}^2(\nu) \tag{28}$$

where $\mathrm{WS}_i(\nu)$ is the value of the Wiener spectrum of the input at ν and $\mathrm{MTF}(\nu)$ is the value of the film's MTF at that frequency. The information capacity thus depends on the frequency response and noise of the system, as would be expected. The matter is discussed by Dainty and Shaw.[52]

Downloaded from Digital Engineering Library @ McGraw-Hill (www.accessengineeringlibrary.com)
Copyright © 2010 The McGraw-Hill Companies. All rights reserved.
Any use is subject to the Terms of Use as given at the website.

29.21 LIST OF PHOTOGRAPHIC MANUFACTURERS

Agfa Photo Division
Agfa Corporation
100 Challenger Road
Ridgefield, NJ 07660

Ilford Photo Corporation
70 West Century Boulevard
Paramus, NJ 07653

E. I. duPont de Nemours and Co.
Imaging Systems Department
666 Driving Park Avenue
Rochester, NY 14613

3M Company
Photo Color Systems Division
3M Center
St. Paul, MN 55144–1000

Eastman Kodak Co.
343 State Street
Rochester, NY 14650
Tel. 1–800–242–2424 for product info.

Polaroid Corporation
784 Memorial Drive
Cambridge, MA 02139
Tel. 1–800–255–1618 for product info.

Fuji Photo Film USA
555 Taxter Road
Elmsford, NY 10523

29.22 REFERENCES

1. W. Thomas (ed.), *SPSE Handbook of Photographic Science and Engineering*, Wiley, New York, 1973, sec. 8.
2. B. H. Carroll, G. C. Higgins, and T. H. James, *Introduction to Photographic Theory*, Wiley, New York, 1980, chaps. 6–9.
3. T. H. James (ed.), *The Theory of the Photographic Process*, 4th ed., Macmillan, New York, 1977.
4. J. Sturge, Vivian Walworth, and Alan Shepp (eds.), *Imaging Processes and Materials*, Van Nostrand Reinhold, New York, 1989, chap. 3. (See also Ref. 3, chap. 4.)
5. G. Haist, *Modern Photographic Processing*, vols. I and II, Wiley, New York, 1979.
6. Klaus Hendricks, chap. 20 of Ref. 4.
7. J. H. Altman, F. Grum, and C. N. Nelson, *Phot. Sci. Eng.* **17:**513 (1973).
8. Reference 3, chaps. IV–VII.
9. *ANSI/ISO*, May 2, 1991. (See also *ANSI/ISO*, May 1, 1984, which sets forth standardized terminology.)
10. R. W. G. Hunt, *The Reproduction of Colour*, 4th ed., Fountain Press, Tolworth, England, 1987, pp. 247–257.
11. *American National Standard*, ANSI PH2.2, 1984, R1989, PH2.17 1985.
12. C. J. Niederpruem, C. N. Nelson, and J. A. C. Yule, *Phot. Sci. Eng.* **10**:35 (1966).
13. *American National Standard*, ANSI PH3.49, 1971, R1987.
14. H. N. Todd and R. D. Zakia, *Phot. Sci. Eng.* **8**:249 (1964). (See also publications of the American National Standards Institute.)
15. M. Hercher and B. J. Ruff, *J. Opt. Soc. Am.* **57**:103 (1967).
16. W. F. Berg, *Proc. Roy. Soc. of London*, ser. A, **174**:5599 (1940).
17. Reference 2, p. 141.
18. *Scientific Imaging with Kodak Films and Plates*, Publication P315, Eastman Kodak Co., Rochester, N.Y., 1987, p. 63.
19. J. Kapecki and J. Rodgers, *Kirk-Othmer Encyclopedia of Chemical Technology*, 4th ed., vol. 6,Wiley, New York, 1993, p. 965.
20. S. H. Liggero, K. J. McCarthy, and J. A. Stella, *J. Imaging Technology* **10**:1 (1984).

Downloaded from Digital Engineering Library @ McGraw-Hill (www.accessengineeringlibrary.com)
Copyright © 2010 The McGraw-Hill Companies. All rights reserved.
Any use is subject to the Terms of Use as given at the website.

21. Reference 5, chap. 7.
22. E. H. Land, *Phot. Sci. Eng.* **16**:247 (1972).
23. Reference 10, chap. 11 et seq.
24. See, for example, F. R. Clapper in Ref. 3, sec. II, chap. 19.
25. R. M. Evans, *Eye, Film, and Camera in Color Photography*, Wiley, New York, 1959, p. 180.
26. B. J. Thompson, *Progress in Optics VII*, E. Wolf (ed.), North-Holland Publishing Co., Amsterdam, 1969; R. E. Swing, *J. Opt. Soc. Am.* **62**:199 (1972); Dainty and Shaw, Ref. 27, chap. 9.
27. P. Kowalski, *Applied Photographic Theory*, Wiley, New York, p. 77 et seq.
28. C. N. Nelson, Ref. 3, chap. 19.
29. G. C. Higgins and L. A. Jones, *J. Soc. of Mot. Pict. & TV Engrs.* **58:**277 (1952).
30. J. Gasper and J. J. dePalma, Ref. 3, chap. 20.
31. J. C. Dainty and R. Shaw, *Image Science*, Academic Press, London, 1974, chaps. 6 and 7. (See also J. C. Dainty, *Optica Ada* **18**:795, 1971.)
32. R. M. Gendron, *J. Soc. of Mot. Pict. & TV Engrs.* **82:**1009 (1973).
33. E. W. H. Selwyn, *Photography Journal* **75**:571 (1935).
34. C. J. Bartleson, *Photography Journal* **33:**117 (1985).
35. K. F. Stultz and H. J. Zweig, *J. Opt. Soc. Am.* **49:**693 (1959).
36. F. W. Sears, *Optics*, Addison-Wesley, Reading, Mass., 1949, p. 159.
37. *American National Standard*, ANSI PH2.40, 1985, R1991.
38. Reference 31, chap. 8.
39. E. C. Doerner, *J. Opt. Soc. Am.* **52:**669 (1962).
40. C. J. Bartleson, *J. Phot. Sci.* **30:**33 (1982).
41. S. Ikenoue and M. Tabei, *J. Imaging Sci.* **34:**187 (1990).
42. Reference 2, p. 335.
43. A. Rose, *J. Mot. Pict. & TV Engrs.* **47:**273 (1946).
44. R. C. Jones, *Phot. Sci. Eng.* **2**:57 (1958).
45. Reference 31, chap. 8, p. 311 et seq.
46. Reference 4, table 3.2, p. 73.
47. G. R. Bird, R. C. Jones, and A. E. Ames, *Appl. Opt.* 2389 (1969).
48. *American National Standard*, ANSI PH2.33, 1983, R1990.
49. O. H. Schade, *J. Soc. Mot. Pict. & TV Engrs.* **73:**81 (1964).
50. J. H. Altman and H. J. Zweig, *Phot. Sci. Eng.* **7:**173 (1963).
51. R. Clark Jones, *J. Opt. Soc. Am.* **51:**1159 (1961).
52. Reference 31, chap. 10.

Downloaded from Digital Engineering Library @ McGraw-Hill (www.accessengineeringlibrary.com)
Copyright © 2010 The McGraw-Hill Companies. All rights reserved.
Any use is subject to the Terms of Use as given at the website.